Am J Transl Res 2021;13(3):1290-1306
www.ajtr.org /ISSN:1943-8141/AJTR0118598

Original Article

Schistosoma japonicum-derived peptide SJMHE1 promotes peripheral nerve repair through a macrophage-dependent mechanism

Yongbin Ma[1,2], Chuan Wei[1], Xin Qi[1], Yanan Pu[1], Liyang Dong[3], Lei Xu[1], Sha Zhou[1], Jifeng Zhu[1], Xiaojun Chen[1], Xuefeng Wang[4], Chuan Su[1]

[1]State Key Lab of Reproductive Medicine, Jiangsu Key Laboratory of Pathogen Biology, Department of Pathogen Biology and Immunology, Center for Global Health, Nanjing Medical University, Nanjing 211166, Jiangsu, P. R. China; [2]Department of Neurology Laboratory, Jintan Hospital, Jiangsu University, Jintan, Changzhou 213200, Jiangsu, P. R. China; [3]Department of Nuclear Medicine and Institute of Oncology, The Affiliated Hospital of Jiangsu University, Zhenjiang 212000, Jiangsu, P. R. China; [4]Department of Central Laboratory, The Affiliated Hospital of Jiangsu University, Zhenjiang 212000, Jiangsu, P. R. China

Received July 21, 2020; Accepted December 11, 2020; Epub March 15, 2021; Published March 30, 2021

Abstract: Peripheral nerve injury, a disease that affects 1 million people worldwide every year, occurs when peripheral nerves are destroyed by injury, systemic illness, infection, or an inherited disorder. Indeed, repair of damaged peripheral nerves is predominantly mediated by type 2 immune responses. Given that helminth parasites induce type 2 immune responses in hosts, we wondered whether helminths or helminth-derived molecules might have the potential to improve peripheral nerve repair. Here, we demonstrated that schistosome-derived SJMHE1 promoted peripheral myelin growth and functional regeneration via a macrophage-dependent mechanism and simultaneously increased the induction of M2 macrophages. Our findings highlight the therapeutic potential of schistosome-derived SJMHE1 for improving peripheral nerve repair.

Keywords: Peripheral nerve regeneration, neuroregeneration, myelination, macrophage

Introduction

Peripheral neuropathy is a common neurological disorder resulting from peripheral nerve injury that occurs when the peripheral nerves are destroyed by injury, systemic illness, infection, or an inherited disorder. Although the peripheral nervous system maintains regenerative ability, this regeneration occurs at a slow rate and is inefficient when myelin sheaths are thinner, leading to sensory and motor dysfunction, neuropathic pain, and even permanent disability [1-3]. These disastrous consequences not only reduce the quality of life of patients but also impose very large social and economic burdens [4]. However, an effective therapeutic strategy for promoting nerve regeneration and functional rehabilitation is still lacking.

Repair of peripheral nerve injury depends on the events of Wallerian degeneration distal to the lesion site [5]. Importantly, Wallerian degeneration is predominantly orchestrated by the immune response, which involves several immune cells, including dendritic cells, T cells, B cells, and particular macrophages [6-8]. Indeed, Wallerian degeneration is largely dominated by macrophages, which not only inhibit proinflammatory factors but also help to remove myelin debris, regulate glial cell activity, and secrete various bioactive factors to promote damaged nerve regeneration [9-11]. Similar to other types of tissue repair [12, 13], damaged peripheral nerve repair is likely to be mediated by type 2 immunity, such as the Th2 cell response and M2 macrophage response [14, 15], which mediate tissue repair both by limiting inflammation and by directly inducing reconstruction of the damaged tissue [16]. Thus, manipulation of type 2 immunity, particularly the M2 macrophage response, is a promising therapeutic strategy for peripheral nerve injury [17-19].

Parasitic helminths elicit strong type 2 immune responses, which play a pivotal role in mediating both host resistance (e.g., the expulsion of helminths and prevention of reinfection) and disease tolerance (e.g., control of inflammation and tissue repair) mechanisms [20]. Based on this, we postulated that helminth-derived molecules might have therapeutic potential to improve tissue repair through inducing the tissue repair-associated type 2 immune response, particularly the M2 macrophage cell-mediated response. Consistent with this notion, published data have shown that liver fluke-derived granulin peptide can improve diabetic wound healing [21]. However, whether helminths or helminth-derived molecules can promote damaged peripheral nerve repair remains unknown.

In this study, we found that the peptide SJMHE1 derived from a helminth, *Schistosoma japonicum* [22], promoted peripheral myelin growth and functional regeneration after sciatic nerve injury in a macrophage-dependent and M2-related manner. Our findings propose a promising pharmaceutical agent for the treatment of peripheral nerve injury.

Materials and methods

SJMHE1 peptide

The peptide SJMHE1 from SjHSP60 437-460 (VPGGGTALLRCIPVLDTLSTKNED) was synthesized and analyzed by high-performance hydraulic chromatography to obtain an accurate measurement of peptide content (Top-peptide, Shanghai, China). LPS contamination was avoided by pretreatment with polymyxin B-agarose. The dose of SJMHE1 peptide we used in this study was based on the single therapeutic dose (10 μg) used in our previous study [23].

Animals and surgical procedures

Adult male Sprague-Dawley rats (body weight: 220 ± 10 g) were purchased and reared in the Animal Experimental Center of Jiangsu University in a standardized environment consisting of a 12 h light/dark cycle, sterile water, standard pellet feed, and sterile bedding. All animal experiments were conducted in accordance with the Guidelines for the Protection and Use of Experimental Animals and the Measures for the Administration of Animal Use at Jiangsu University and were reviewed and approved by the Animal Ethics Committee of Jiangsu University (permit number: UJS-IACUC-2018030120).

Thirty-six rats were randomly divided into 3 groups (n = 12 in each group): the normal group, control group (PBS), and SJMHE1 treatment group. All rats were anesthetized by an intraperitoneal injection of pentobarbital sodium (50 mg/kg; Sigma, St. Louis, MO, USA). Subsequently, the rats were fixed on the operating table in a prone position, their left hind legs were shaved, and iodophor was used to disinfect the skin to ensure sterility. The sciatic nerve was exposed through an incision in the left hind limb, and 3 mm long of the nerve was excised. The nerve stumps (proximal end and distal end) were each retracted 1 mm to form a 5 mm gap. A 7-mm long silicone tube (inner diameter: 1 mm; Helix Medical, Carpinteria, CA, USA) was implanted to bridge the nerve gap, and the the proximal and distal nerve stumps were inserted into the lumen at a depth of 1 mm and anastomosed by 10-0 nylon sutures. Then, PBS or SJMHE1 (10 μg) was mixed with matrix glue (BD Biosciences, Billerica, MA) uniformly at a volume ratio of 1:1. Precooled microsyringes were used for injection into the lumen and stump from the anastomoses on both sides. The injection was performed as slowly as possible to avoid the formation of air bubbles. Thereafter, the muscle and skin were sutured with 4-0 nylon sutures. After the operation, the rats were kept in a large cage with sawdust to minimize discomfort and pain caused by mechanical stimulation. In addition, the rats were checked often for self-mutilation.

Functional evaluation

The functional recovery of rats was evaluated on the 35th day after surgery. Only rats that exhibited no signs of self-harm were evaluated, and researchers who did not participate in the surgical procedure or experimental grouping performed the evaluation according to a previously described method [24, 25]. Briefly, the hind paws were soaked in red ink, the animals were allowed to walk on 30 × 7 cm drawing paper, and 3-5 clearly visible footprints were collected. From the footprints, the following parameters were calculated: the distance from the heel to the third toe (PL) and the distance

from the first toe to the fifth toe (TS). E and N represented the surgical side and the normal side, respectively. The sciatic nerve function index (SFI) was calculated according to the following formula, with 0 indicating normal function and -100 indicating a complete loss of function: SFI = 118.9 × (ETS-NTS/NTS)-51.2 × (EPL-NPL)/NPL-7.5.

Weight ratio and morphology of the gastrocnemius muscle

The rats were sacrificed on the 60th day after the operation. The soleus muscle adjacent to the operated side and the contralateral gastrocnemius muscle were dissected and weighed with an electronic balance. The = ratio of the weight of the gastrocnemius muscle (g) on the operated side to the weight of the contralateral gastrocnemius muscle (g) was calculated to determine the mass of muscle recovered by motor axon reinnervation. Then, the gastrocnemius muscle was fixed with 4% paraformaldehyde, paraffin-embedded, sectioned, and stained with hematoxylin and eosin (H&E). Images were collected using an ECLIPSE E100 microscope (Nikon, Tokyo, Japan).

Nerve tissue preparation

After the rats were sacrificed on the 35th day, the nerve conduits were collected, fixed with 4% paraformaldehyde, embedded in paraffin, and sectioned from the middle point of the nerve conduits for subsequent experiments.

Immunofluorescence

Immunofluorescence was performed using previously reported standard methods [24]. In brief, nerve tissue sections were incubated with rabbit anti-NF200 (1:200, Cat. No: GB13141, Servicebio, Wuhan, China), rabbit anti-S100 (1:200, Cat. No: GB11359, Servicebio), goat anti-CCR7 (1:200, Cat. No: NB100-712SS, Novus Biologicals, Colorado, CO), goat anti-CD206 (1:200, Cat. No: ab64693, Abcam, Cambridge, MA) and rabbit anti-CD68 (1:200, Cat. No: BA3638, Boster, Wuhan, China) antibodies at 4°C overnight. The slices were then incubated with Alexa Fluor 488-conjugated goat anti-rabbit (1:400, Cat. No: GB25303, Servibio), Cy3-conjugated goat anti-rabbit (1:300, Cat. No: GB23303, Servibio), FITC-conjugated donkey anti-goat (1:200, Cat. No: GB21404, Servibio), HRP-conjugated goat anti-rabbit (1:500, Cat. No: GB21303, Servibio), and Cy3-conjugated donkey anti-rabbit (1:300, Cat. No: GB21403, Servibio) secondary antibodies for 1 h. The nuclei were stained with DAPI (5 μg/mL) for 10 min, and then the sections were observed with an ECLIPSE C1 (Nikon) fluorescence microscope. The fluorescence intensity of 6 random pictures captured from each slice was measured by using Image-Pro Plus software (Version X, Adobe, San Jose, CA).

Transmission electron microscopy

Transmission electron microscopy was performed as previously described [24]. Nerve tissue catheters were harvested on the 35th day, fixed in 2.5% glutaraldehyde for 24 h, dehydrated, embedded with EPDN-812, and sliced. Then, the sections were stained with uranyl acetate and lead citrate for 20 min, and pictures were taken with an HT7700 transmission electron microscope to observe the ultrastructure, thickness, and number of myelin sheaths.

Schwann cell culture and determination of proliferation and migration

Schwann cells were isolated and purified by enzymatic digestion of the sciatic nerves of 3-day-old SD rats according to a previously described standard procedure [26]. P4 or P5 Schwann cells were identified by immunofluorescence staining using GFAP (1:200, Cat. No: GB11096, Servibio) and S100 (1:200, Cat. No: GB11359, Servibio) antibodies, and Schwann cells with a purity greater than 98% were used in this experiment. Schwann cells were digested and seeded into 96-well plates, treated with SJMHE1 peptide at different concentrations (0.1 μg/ml, 1 μg/ml, or 10 μg/ml) and cultured for 24 h. According to the manufacturer's instructions, the proliferative ability of the Schwann cells was measured using a CCK-8 assay kit. In a 24-well plate, Schwann cells were pretreated with different concentrations (0.1 μg/ml, 1 μg/ml, or 10 μg/ml) of SJMHE1 peptide. Then, Ki67 immunofluorescence staining was performed to further evaluate the proliferative ability of Schwann cells. A rabbit anti-Ki67 primary antibody (1:200, Cat. No: GB13030-2, Servibio) and Cy3-conjugated goat anti-rabbit secondary antibody (1:200, Cat. No: GB23303, Servibio) were used.

In a 6-well plate, Schwann cells were pretreated with different concentrations (0.1 μg/ml, 1 μg/ml, or 10 μg/ml) of SJMHE1 peptide. Then, 1×10^5 Schwann cells were suspended in 100 μL serum-free culture medium and seeded in the upper chamber of a Transwell system (Costar, Cambridge, MA), the lower chamber of the Transwell system was filled with 600 μL complete culture medium for 12 h, and the cells were stained with 0.1% crystal violet. An ICC50 HD microscope was used for image acquisition and counting (Leica Microsystems).

Isolation and culture of dorsal root ganglia

Dorsal root ganglia (DRGs) were obtained according to a previous method with minor modifications [27]. Briefly, 3-day-old SD rats were sacrificed. The vertebral body was sectioned along the sagittal plane, the DRGs were removed one by one from the intervertebral foramen, and the outer membrane was peeled off under a microscope. The DRGs were placed in a 24-well plate coated with polylysine and cultured in neurobasal medium (Gibco, Carlsbad, CA) supplemented with 2% B27 (Invitrogen), 50 ng/mL NGF (Invitrogen), 2 mmol/L-glutamine (Invitrogen), and 1% cyan-streptomycin. The next day, SJMHE1 peptide was added at different concentrations (0.1 μg/ml, 1 μg/ml, or 10 μg/ml SJMHE1) for 4 days. A rabbit anti-tubulin β-III primary antibody (1:200, Cat. No: GB11139, Servibio) and Cy3-conjugated goat anti-rabbit secondary antibody (1:300, Cat. No: GB23303, Servibio) were used for fluorescence staining, and the morphology of DRG spheres and regenerated axons of individual neurons were observed using an ECLIPSE C1 (Nikon) fluorescence microscope. In all experiments, the DRGs were treated with 10 μm cytarabine (Sigma) to remove non-nerve cells.

Chlorophosphate liposome study

A chlorophosphate liposome suspension (F70-101C-A, Palo Alto, CA) and negative control (F70101-A) were purchased from FormuMAX Scientific. To prevent liposome precipitation, the suspension was shaken and mixed evenly before use to ensure homogenization. In this experiment, on the basis of a previous description protocol [11], local injection into the nerve conduit and stump effectively depleted resident macrophages and some peripheral circulating macrophages. The experimental group included two groups (n = 6 in each group): the liposome (negative control) + SJMHE1 group and chlorophosphate liposome group + SJMHE1 group. The specific details of the procedure were consistent with the model construction and injection protocols described above. On the 10th day after the operation, the rats were killed to collect nerve conduits, which were fixed with 4% paraformaldehyde, paraffin-embedded, and sectioned. Rabbit anti-tubulin β-III (1:200, Cat. No: GB11139, Servibio) and rabbit anti-CD68 primary antibodies (1:200, Cat. No: BA3638, Boster) and Alexa Fluor 488-conjugated goat anti-rabbit (1:400, Cat. No: GB25303, Servibio) and Cy3-conjugated goat anti-rabbit secondary antibodies (1:300, Cat. No: GB23303, Servibio) were used for immunofluorescence staining, and an ECLIPSE C1 (Nikon) fluorescence microscope was used to observe the morphology.

According to the manufacturer's instructions, clodronate was encapsulated in liposomes at a concentration of 7 mg/ml. To study the effect of chlorophosphate liposomes on Schwann cells, Schwann cells were seeded in 96-well plates overnight. Then, the culture medium was replaced with 200 μl complete medium containing different concentrations of chlorophosphate liposomes (21.857 μg/ml, 43.75 μg/ml, 87.5 μg/ml, or 175 μg/ml) per well in a 96-well plate, and the cells were cultured for 24 h and 48 h. The proliferation of Schwann cells was assessed by the CCK8 assay. The concentrations were selected based on the in vivo dose of 5 μl (35 μg).

Culture and treatment of RAW264.7 cells

The mouse macrophage line RAW264.7 was purchased from ATCC (Manassas, VA). RAW-264.7 cells were cultured in DMEM containing 10% fetal bovine serum and 1% cyan-streptomycin and incubated in 5% CO_2 at 37°C. According to previous studies [28], RAW264.7 cells were pretreated with 0.1 μg/ml SJMHE1 peptide for 24 h. Then, fluorescence staining was performed using mouse anti-iNOS (1:200, Cat. No: ab49999, Abcam) and rabbit anti-Arg1 (1:200, Cat. No: ab91279, Abcam) primary antibodies and Alexa Fluor 647-conjugated goat anti-mouse (1:500, Abcam) and Alexa Fluor 488-conjugated donkey anti-rabbit (1:500, Abcam) secondary antibodies.

To study the effect of SJMHE1 on the proliferation of macrophages, RAW264.7 cells were pretreated with SJMHE1 at different concentrations (0.1 μg/ml, 1 μg/ml, and or 10 μg/ml). Then, the cells were digested and seeded in 96-well and 24-well plates for 24 h and 48 h. The CCK8 assay and Ki67 immunofluorescence staining were performed to evaluate the proliferation of RAW264.7 cells.

To study the effect of SJMHE1 on the migration of macrophages, a scratch wound assay was performed to assess the migration of RAW-264.7 cells. Briefly, RAW264.7 cells were plated in a 6-well plate. When the cell confluence reached 80%, the monolayer was scratched vertically with a pipette tip, and the plate was washed with PBS to remove the detached cells. Then, the cells were cultured in complete medium supplemented with SJMHE1 for 24 h. The cells were monitored and photographed at multiple sites at 0 and 24 h. Images were captured using a CKX-53 microscope (Olympus, Tokyo, Japan). Wound healing was calculated as follows: (distance from the scratch at 0 h -distance of cell migration at 24 h/distance from the scratch at 0 h) × 100%.

Western blot analysis

Briefly, after pretreatment with 0.1 μg/ml SJMHE1 peptide or 1 μg/ml LPS for 24 h, the cells were collected and lysed in RIPA buffer (Cell Signaling Technology, Danvers, MA) containing PMSF (Beyotime, Nantong, China) and quantified using a BCA Protein Assay Kit (Beyotime). Equal amounts of protein (50 μg) were separated by 10% sodium dodecyl sulfate-polyimide gel electrophoresis (SDS-PAGE) and transferred to polyvinylidene fluoride membranes (Bio-Rad, Hercules, CA). Then, the membranes were blocked with 5% BSA and incubated with mouse anti-iNOS (1:1000, Cat. No: ab49999, Abcam) and rabbit anti-Arg 1 (1: 1000, Cat. No: ab91279, Abcam) primary antibodies at 4°C overnight. The membranes were then incubated with an HRP-conjugated secondary antibody for 1 h. The bands were visualized using an ECL chemiluminescence kit.

Extraction and treatment with conditioned medium

Briefly, RAW264.7 cells were cultured in complete medium containing 0.1 μg/ml SJMHE1 for 24 h. Then, the medium was replaced with serum-free medium, the cells were cultured for 24 h, and the supernatant was collected. Schwann cells and DRG neurons were treated with the collected supernatant. The proliferation of Schwann cells was evaluated by the CCK8 assay, and the morphological characteristics of DRG neurons were assessed by tubulin β-III immunofluorescence staining.

Statistical analysis

GraphPad Prism 5.0 (La Jolla, CA) was used for statistical analysis, and the data are expressed as the mean ± SEM. Differences between two groups were analyzed by unpaired two-tailed Student's *t* test, and those between three or more groups were analyzed by ANOVA. A value of $P<0.05$ was considered statistically significant.

Results

SJMHE1 peptide promoted functional recovery after peripheral nerve injury

To evaluate whether SJMHE1 has a therapeutic effect on peripheral nerve injury, we transfected the sciatic nerves of the left hindlimbs of adult male Sprague-Dawley rats and then treated these rats with SJMHE1 or PBS. The results showed that both the spreading of the plantar surface of the hind paw (**Figure 1A**) and the SFI value (**Figure 1B** and **1C**) of SJMHE1-treated rats were significantly better than those of control rats, suggesting the recovery of motor function after SJMHE1 treatment. Furthermore, atrophy of the gastrocnemius muscle was significantly alleviated and the wet weight ratio of the gastrocnemius muscle was significantly improved in SJMHE1-treated rats (**Figure 1D-F**). Taken together, these results indicate that schistosome-derived SJMHE1 enhances functional recovery after sciatic nerve injury.

SJMHE1-mediated peripheral nerve repair was associated with increased myelin sheath regeneration

In parallel with improved functional recovery, the regenerated sciatic nerve was thicker in SJMHE1-treated rats than in control rats (**Figure 2A**). We next performed S100 and NF200 coimmunofluorescence staining to determine the effect of SJMHE1 on the regeneration of

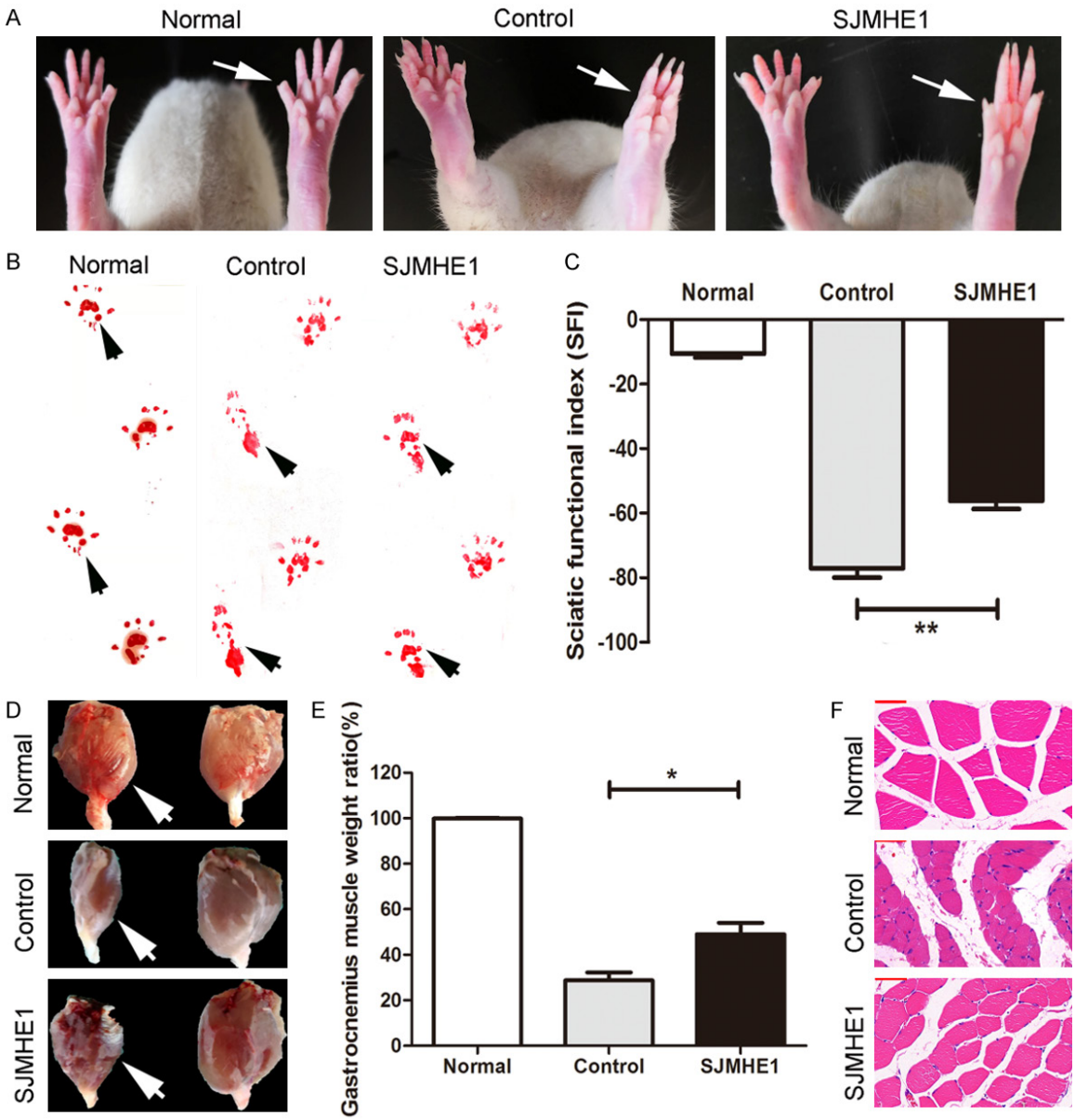

Figure 1. SJMHE1 promoted functional recovery after sciatic nerve transection in rats. A. Toe spreading 35 days after sciatic nerve transection. B. Representative photographs of rat footprints. C. Statistical analysis of the sciatic nerve function index (SFI). D. Morphological characteristics of the gastrocnemius muscle 60 days after sciatic nerve transection. E. Statistical analysis of the gastrocnemius muscle wet weight ratio. F. Representative photographs of H&E staining of cross-sections of gastrocnemius muscles. Scale bar = 50 μm. The arrows in all pictures indicate the operated side. The SJMHE1 group *vs* the control group; n = 6 for each group; **P*<0.05, ***P*<0.01 (ANOVA). The data are presented as the mean ± SEM.

myelinated fibers. The results showed that SJMHE1 treatment promoted the regeneration of the myelin sheath, which was reflected by increased expression of both S100 and NF200 (**Figure 2B-D**). In addition, the thickness and number of myelin sheaths were significantly increased in SJMHE1-treated rats (**Figure 2E-G**). These results suggest that SJMHE1 treatment enhances the regeneration of the myelin sheath.

SJMHE1 had no direct effect on Schwann cells and DRG

To determine whether SJMHE1 promoted myelin sheath regeneration through directly tar-

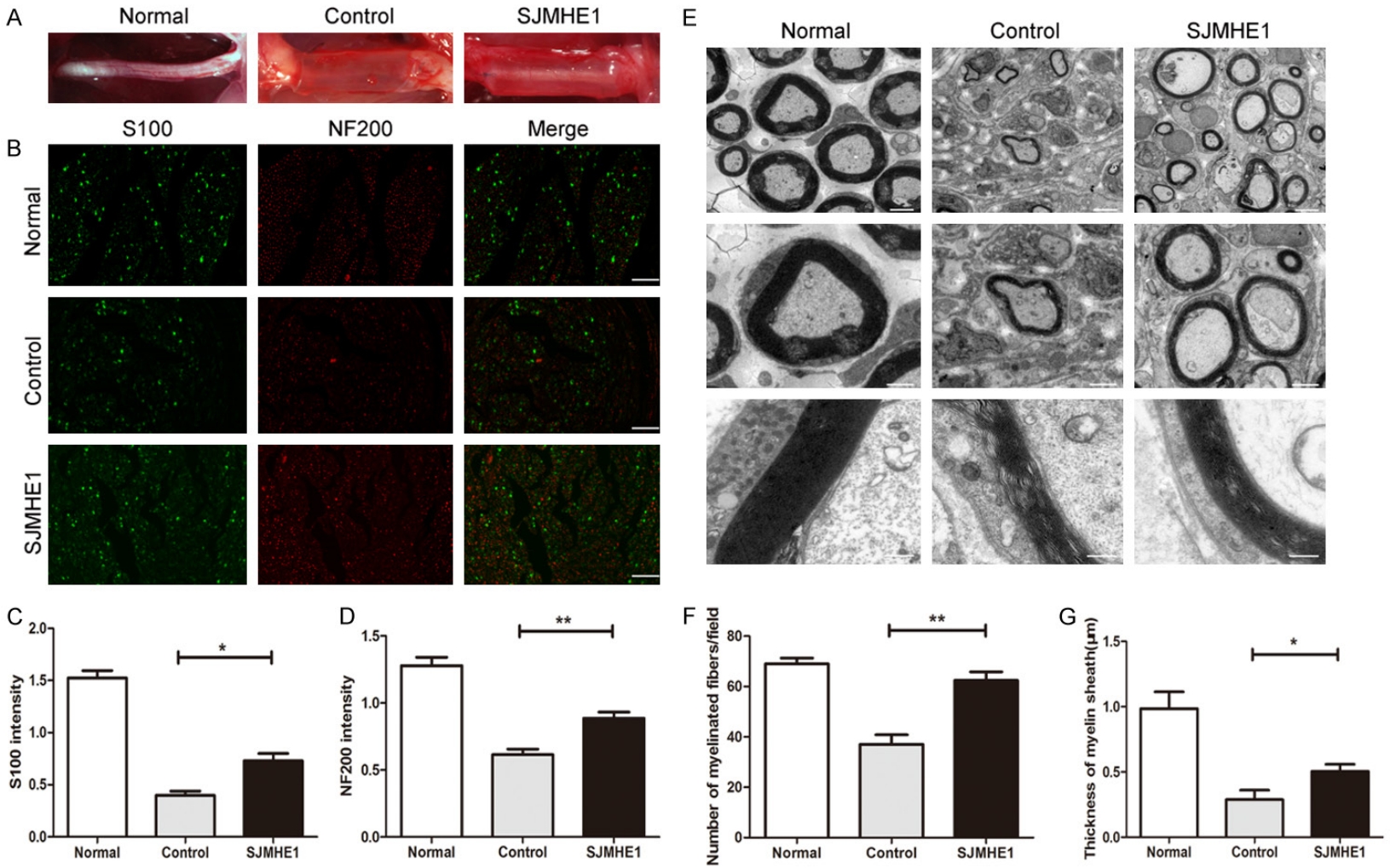

Figure 2. SJMHE1 promoted nerve regeneration after sciatic nerve transection in rats. A. Morphological characteristics of regenerated nerves in nerve conduits 35 days after sciatic nerve transection. B. Double immunofluorescence staining for S100 (green) and NF200 (red) in cross-sections of the regenerated nerve region at the midpoint of the nerve conduit. Scale bar = 50 μm. C, D. Quantitative analyses of the fluorescence intensity of S100 and NF-200. E. TEM images of cross-sections of the regenerated nerve region at the midpoint of the nerve conduit. The scale bars in each group from top to bottom are as follows: 20 μm, 5 μm, and 1 μm. F, G. Statistical analysis of the myelin sheath number and myelin sheath thickness. The SJMHE1 group *vs* the control group; n = 6 for each group; **P*<0.05, ***P*<0.01 (ANOVA). The data are presented as the mean ± SEM.

geting Schwann cells, Schwann cells were isolated (**Figure 3A**). The CCK8 assay and Ki67 staining showed that SJMHE1 had no demonstrable direct effect on Schwann cell proliferation or migration *in vitro* (**Figure 3B-F**). In addition, the lengths of the nerve filaments of SJMHE1-treated DRG neuron axons and single neuron axons were similar to those of PBS-treated DRG neuron axons (**Figure 3G** and **3H**). Thus, these results show that schistosome-derived SJMHE1 has no detectable direct effect on the proliferation and migration of Schwann cells or the growth of axons.

SJMHE1 promoted sciatic nerve repair via a macrophage-dependent mechanism

Given the central role of macrophages in peripheral nerve repair, we next wondered whether macrophages were involved in SJMHE1-mediated sciatic nerve repair. Nerve conduits were collected, and immunofluorescence staining of CD68 was performed. As expected, the number of macrophages was significantly increased in regenerated nerve tissue from SJMHE1-treated rats, as shown by increased CD68 expression (**Figure 4A** and **4B**). More importantly, chlorophosphate liposomes were locally injected to deplete macrophages in injured sciatic nerve tissue (**Figure 4C** and **4D**). The results showed that macrophage depletion abrogated the SJMHE1-induced improvement in sciatic nerve repair, as indicated by the lengths of the regenerated axons (**Figure 4E** and **4F**). However, chlorophosphate liposomes had no effect on the proliferative activity of Schwann cells *in vitro* (Supplementary Figure 1). Furthermore, we found that conditioned medium from macrophages treated with SJMHE1 significantly promoted the proliferative activity of Schwann cells and the growth of DRG neuron axons (Supplementary Figure 2), indicating that macrophages treated with SJMHE1 promoted Schwann cell proliferation and axon growth by producing soluble factors. These results demonstrate that schistosome-derived SJMHE1 enhances injured sciatic nerve repair in a macrophage-dependent manner.

SJMHE1 promoted macrophage migration

To clarify the mechanisms by which SJMHE1 results in an increase in the macrophage population at the injured site, we examined the effect of SJMHE1 on the migration and proliferation of macrophages by the CCK8 assay and Ki67 staining *in vitro*. As shown in **Figure 5A-C**, the proliferation of RAW264.7 cells was not affected by SJMHE1. Next, we performed a wound-healing assay to evaluate the effects of SJMHE1 on macrophage migration and found that SJMHE1 promoted macrophage migration (**Figure 5D** and **5E**). These results demonstrate that SJMHE1 can promote macrophage migration without affecting macrophage proliferation.

SJMHE1 induced proregenerative M2 macrophage polarization

Given that substantial evidence shows that M2 macrophages can promote peripheral nerve regeneration [17-19], we examined the effect of SJMHE1 on the polarization of macrophages in vivo. Strikingly, SJMHE1 treatment increased the number of M2 macrophages ($CD206^+$ $CD68^+$ cells) at the site of the injury and the surroundings while decreasing the number of M1 macrophages ($CCR7^+CD68^+$ cells) in SJMHE1-treated rats (**Figure 6A-D**). To clarify the direct effect of SJMHE1 on M2 macrophage polarization, we treated RAW264.7 macrophages with SJMHE1 *in vitro*. We found that SJMHE1 induced the polarization of macrophages to the M2 phenotype, as indicated by increased expression of Arg-1, a marker of M2 macrophages (**Figure 6E-G**). No detectable iNOS signals were observed in SJMHE1-treated macrophages (**Figure 6E-G**).

Overall, these findings indicate that schistosome-derived SJMHE1 enhances damaged peripheral nerve repair in a macrophage-dependent manner and concomitantly increases M2 macrophage polarization, highlighting the therapeutic potential of SJMHE1 for promoting peripheral nerve repair.

Discussion

Peripheral nerve injury is a common disease caused by injury, systemic illness, infection, or an inherited disorder that may lead to sensory and motor dysfunction, neuropathic pain, or even permanent disability. However, effective therapeutic strategies for enhancing peripheral nerve regeneration and functional recovery are still lacking. Here, we demonstrated that *Schistosoma japonicum*-derived SJMHE1 polypeptide promoted the repair and functional recov-

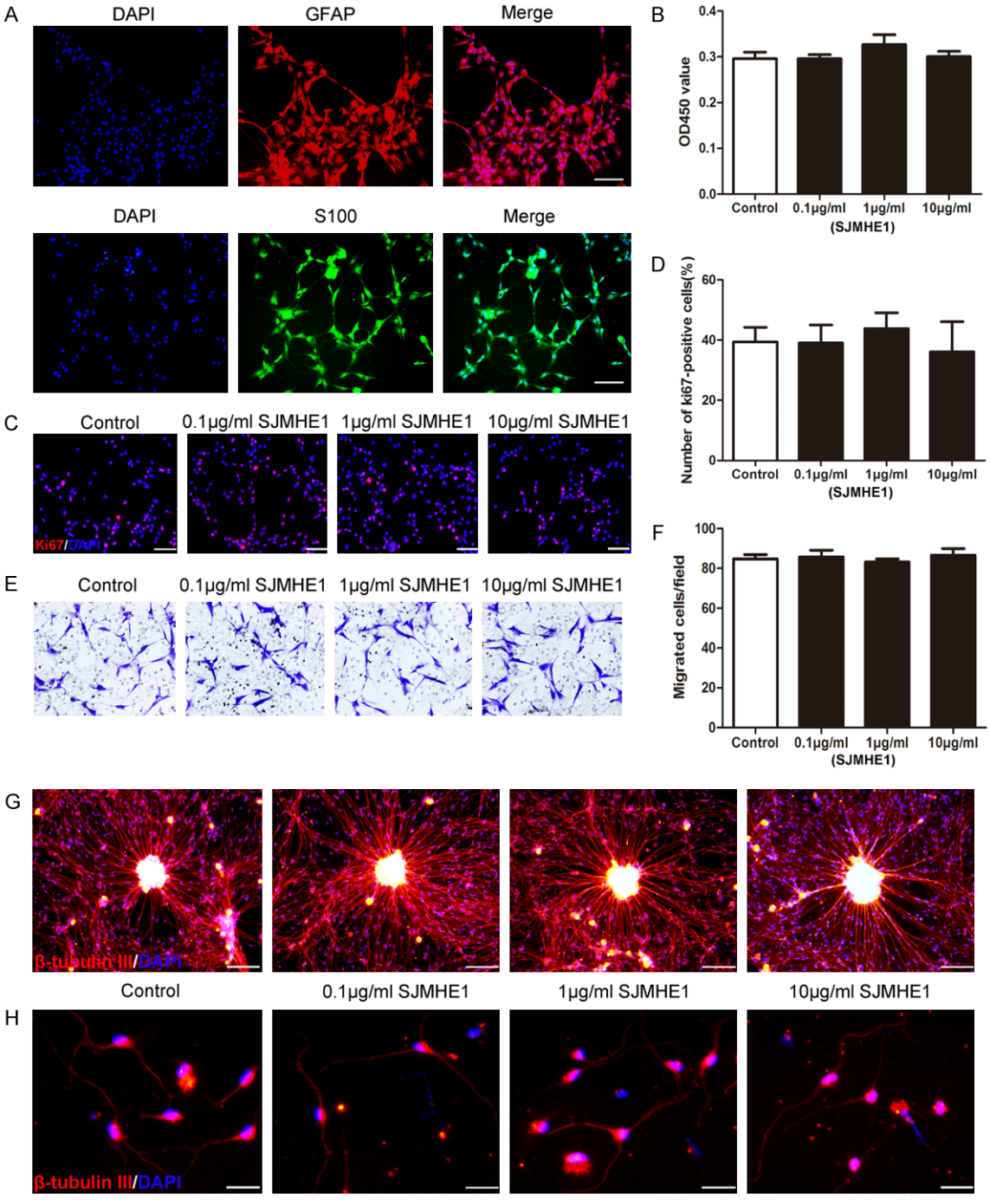

Figure 3. SJMHE1 had no direct effect on the proliferation and migration of Schwann cells or neurite outgrowth of DRGs. A. S100 and GFAP immunofluorescence staining to identify primary Schwann cells. Scale bar = 100 μm. B. Analysis of Schwann cell proliferation by the CCK8 assay. C, D. Assessment of Schwann cell proliferation by Ki67 immunofluorescence staining (red). Scale bar = 100 μm. E, F. Evaluation of Schwann cell migration by the Transwell assay. G, H. Immunofluorescence staining for β-tubulin III (red) in DRGs and single neurons. DAPI (blue)-stained nuclei. Scale bar = 100 μm. Groups treated with different concentrations of SJMHE1 *vs* the control group; n = 3 for each group; $P>0.05$ indicates no statistical significance (ANOVA). The data are presented as the mean ± SEM.

ery of damaged sciatic nerves via a macrophage-dependent mechanism. Our results propose a potential future therapeutic strategy for peripheral nerve injury.

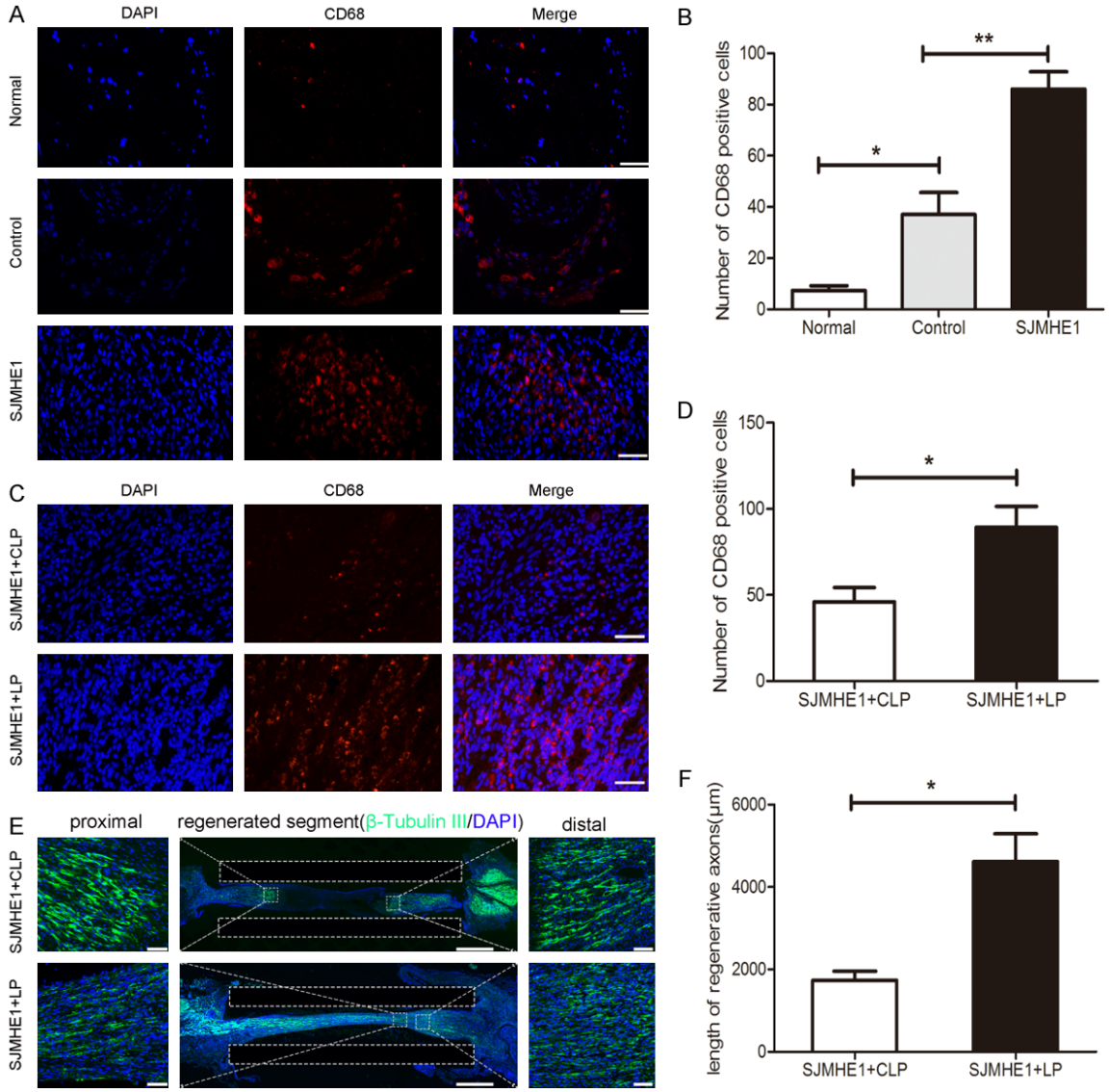

Figure 4. Chlorophosphate liposomes reduced the therapeutic effect of SJMHE1 in an in vivo model. A. Immunofluorescence staining of cross-sections of the regenerated nerve for CD68 (red) 35 days after nerve injury. n = 3. Scale bar = 50 μm. B. Quantitative analysis of the number of CD68-positive cells in different groups. C. Immunofluorescence staining for CD68 (red) in longitudinal sections of the regenerated nerve 10 days after nerve injury. CLP: chlorophosphate liposome. LP: liposome (negative control). n = 6. Scale bar = 50 μm. D. Quantitative analysis of the number of CD68-positive cells in different groups. E. Immunofluorescence staining for β-tubulin III (green) in longitudinal sections of the regenerated nerve. The length of regenerative axons from the proximal end was measured for different groups. Scale bar = 2000 μm. The boxed areas are higher-magnification images. Scale bar = 500 μm. DAPI (blue)-stained nuclei. F. Statistical analysis of the length of regenerative axons. SJMHE1+CLP *vs* SJMHE1+LP; n = 6 for each group; $*P<0.05$, $**P<0.01$ (Student's *t* test; ANOVA). The data are presented as the mean ± SEM.

The therapeutic potential of helminth or helminth-derived molecules has been extensively studied in the context of autoimmune disease alleviation [29, 30]. Given that the inhibition of proinflammatory responses promotes the repair of damaged peripheral nerves [31], it is possible that helminth or helminth-derived molecules also have therapeutic potential for peripheral nerve injury. We found that schistosome-derived SJMHE1 peptide significantly promoted functional recovery and increased axonal regeneration and myelination after sciatic nerve injury. Consistent with these observations, substantial evidence shows that axonal regeneration and myelination are necessary for functional recovery after peripheral nerve

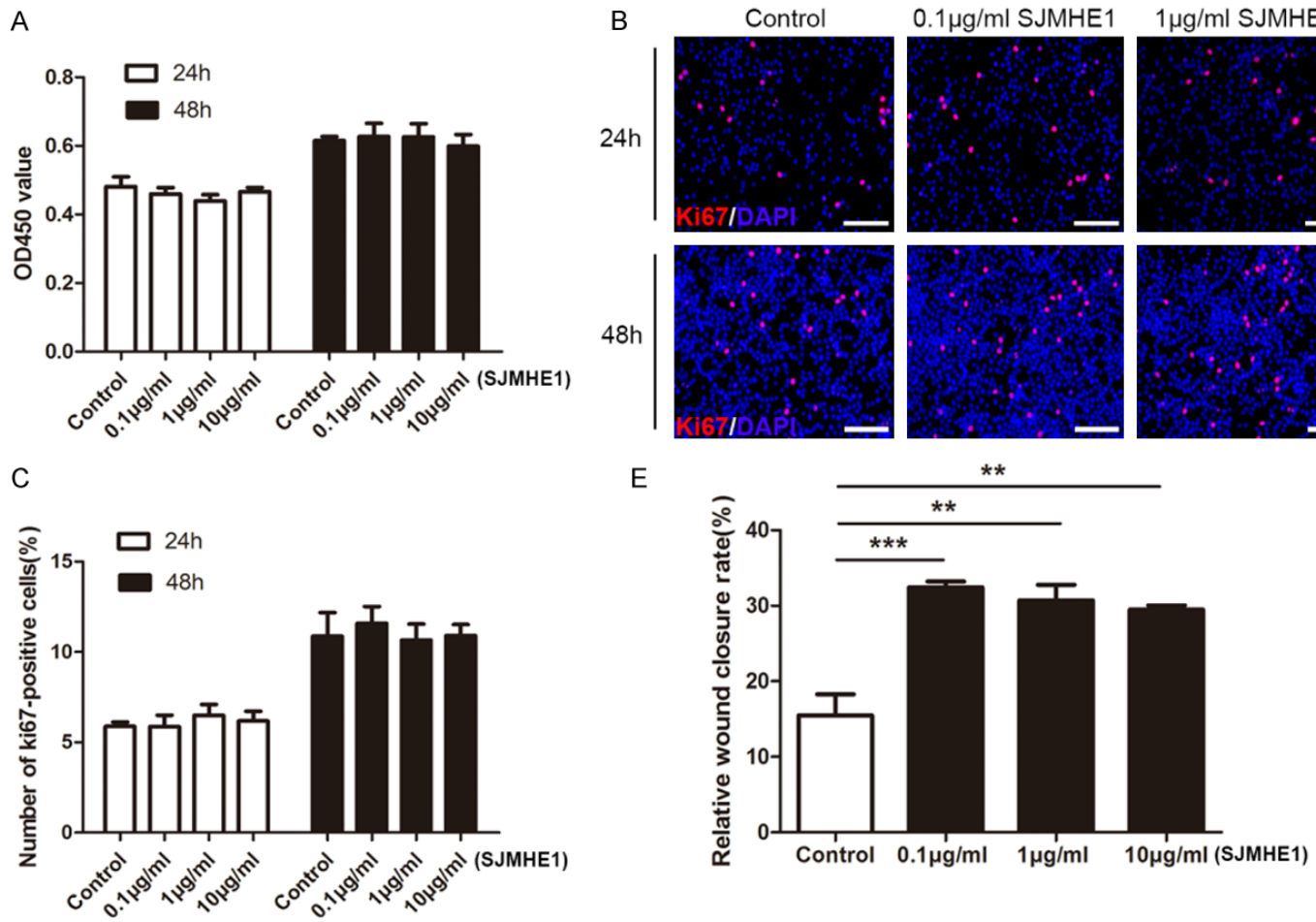
A
24h
48h
OD450 value
0.8
0.6
0.4
0.2
0.0
Control
0.1μg/ml
1μg/ml
10μg/ml
Control
0.1μg/ml
1μg/ml
10μg/ml (SJMHE1)
B
Control
0.1μg/ml SJMHE1
1μg/ml SJMHE1
10μg/ml SJMHE1
24h
48h
Ki67/DAPI
Ki67/DAPI
C
24h
48h
Number of ki67-positive cells(%)
15
10
5
0
Control
0.1μg/ml
1μg/ml
10μg/ml
Control
0.1μg/ml
1μg/ml
10μg/ml (SJMHE1)
E
**
**
***
Relative wound closure rate(%)
40
30
20
10
0
Control
0.1μg/ml
1μg/ml
10μg/ml (SJMHE1)

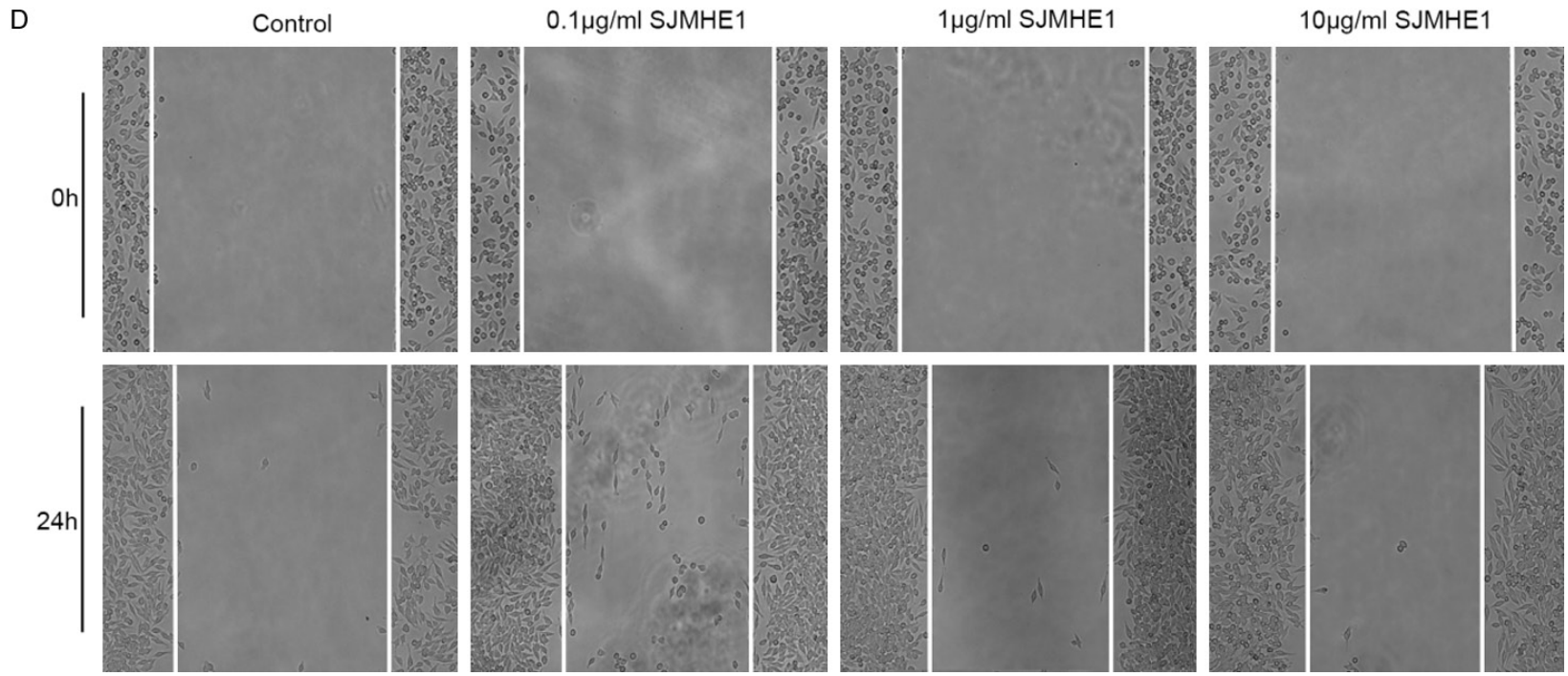

Figure 5. SJMHE1 promoted macrophage migration. A. RAW264.7 cells were incubated with different concentrations of SJMHE1, and cell viability was determined by the CCK8 assay. B, C. Representative images and quantification data of Ki67 staining (red). DAPI (blue)-stained nuclei. Scale bar = 100 μm. D, E. Representative images of and quantification data for the wound-healing assay. Groups treated with different concentrations of SJMHE1 *vs* the control group; n = 3 for each group; $P>0.05$ indicates no statistical significance (ANOVA). The data are presented as the mean ± SEM.

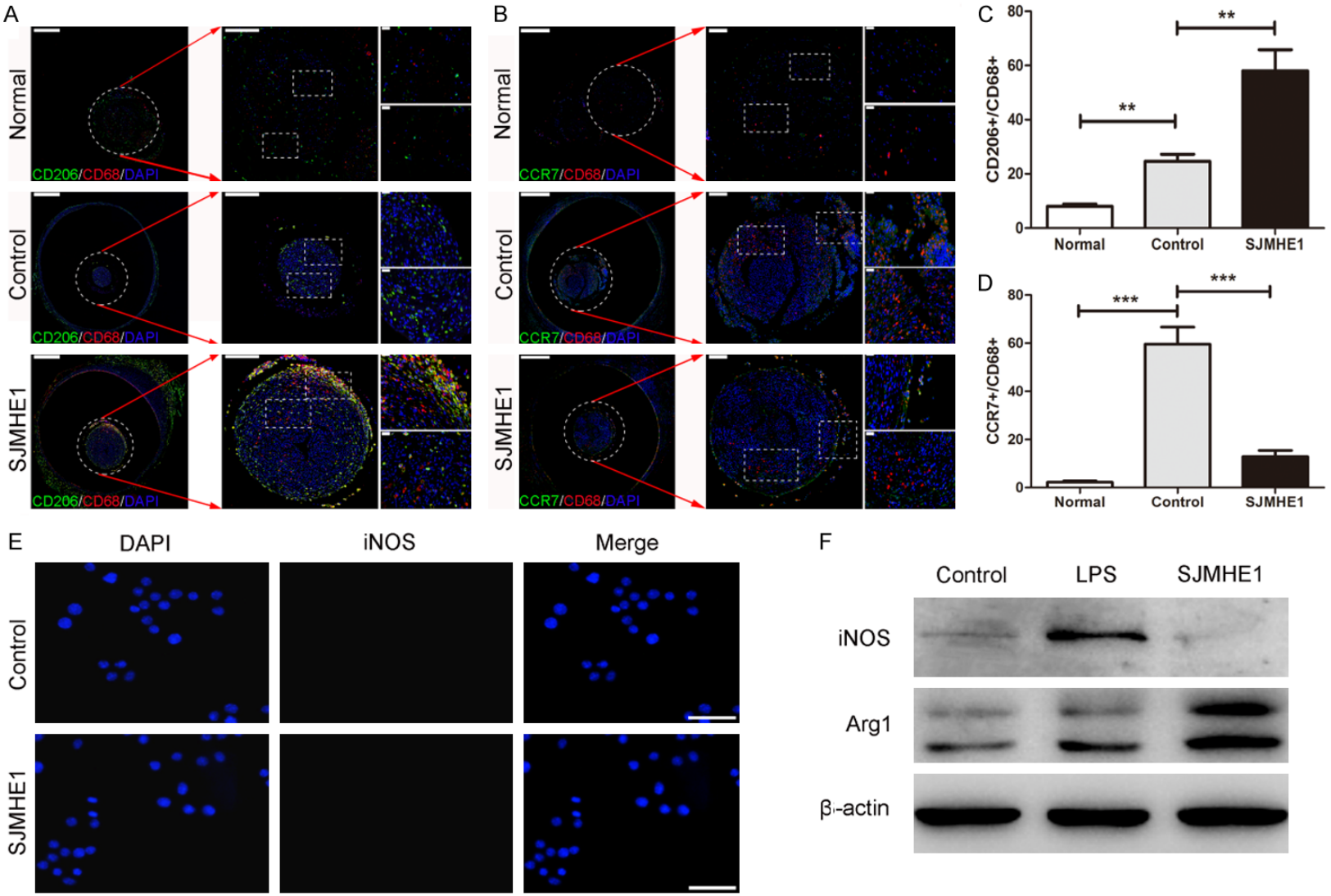
A
Normal
Control
SJMHE1
CD206/CD68/DAPI
B
CCR7/CD68/DAPI
C
CD206+/CD68+
Normal
Control
SJMHE1
**
**
D
CCR7+/CD68+
***
***
E
DAPI
iNOS
Merge
F
Control
LPS
SJMHE1
iNOS
Arg1
β-actin

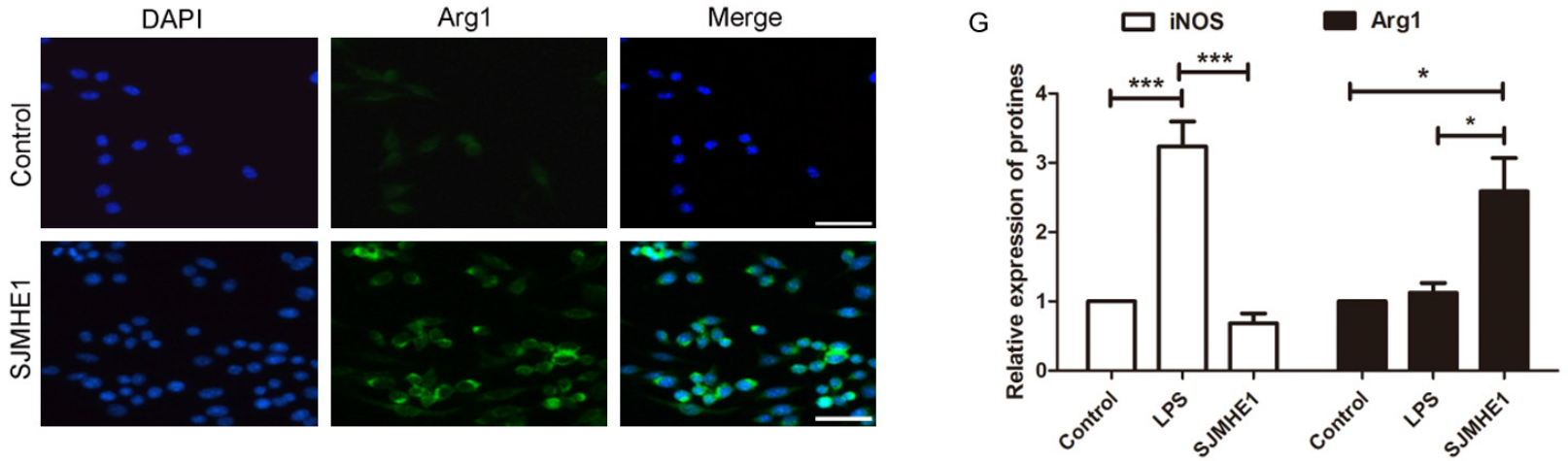

Figure 6. SJMHE1 induced M2 polarization of macrophages. A, B. Images of double immunofluorescence staining of $CD206^+$ (green)/$CD68^+$ (red) and $CCR7^+$ (green)/$CD68^+$ (red) macrophages in cross-sections of the regenerated nerve region at the midpoint of the nerve conduit. Scale bar (left) = 500 μm. The round and boxed areas are higher-magnification images. Scale bar = 200 μm and 20 μm. DAPI (blue)-stained nuclei. C, D. Quantitative analysis of the number of $CD206^+$/$CD68^+$ and $CCR7^+$/$CD68^+$ macrophages in different groups. The ratio of $CD206^+$ cells to $CD68^+$ cells was calculated as the ratio of M2 macrophages. The ratio of $CCR7^+$ cells to $CD68^+$ cells was calculated as the ratio of M1 macrophages. The SJMHE1 group *vs* the control group; n = 6 for each group. E. Immunofluorescence staining of macrophages with the phenotypic markers iNOS and Arg1. DAPI (blue)-stained nuclei. Scale bar = 100 μm. n = 3. F. Western blot analysis of iNOS and Arg1 expression in different groups. The LPS group represents the positive control group. G. Statistical analysis of the relative expression of iNOS and Arg1 proteins. The SJMHE1 group *vs* the control group or LPS group; n = 3 for each group; $*P<0.05$, $**P<0.01$, $***P<0.001$ (ANOVA). The data are presented as the mean ± SEM.

injury [32, 33]. Furthermore, in line with the published data showing that mature Schwann cells play a central role in axonal myelination [34], our results showed that SJMHE1 treatment enhanced Schwann cell maturation, as indicated by a significant increase in S100 expression.

Given that no direct effects of SJMHE1 on Schwann cell proliferation or migration or neurite growth were observed *in vitro*, it is reasonable to hypothesize that SJMHE1 treatment promoted Schwann cell maturation in an indirect manner in vivo after sciatic nerve injury. Notably, macrophage depletion inhibited Schwann cell maturation and subsequently impaired peripheral nerve repair after nerve injury [11], suggesting that macrophages play a key role in Schwann cell maturation. Interestingly, our results showed that macrophage depletion also abrogated the SJMHE1-mediated enhancement of sciatic nerve repair, demonstrating that SJMHE1 promotes damaged peripheral nerve repair in a macrophage-dependent manner. It is well known that M1 macrophages mainly promote inflammation and inhibit the repair of injured peripheral nerves, while M2 macrophages limit inflammation and enhance the repair of injured peripheral nerves [9, 35]. Consistent with this notion, we also found that SJMHE1-mediated promotion of sciatic nerve repair was accompanied by increased percentages and numbers of M2 macrophage. A growing body of evidence indicates that M2 macrophages promote Schwann cell infiltration and axonal growth by producing multiple soluble factors [36, 37]. Consistently, our results showed that conditioned medium from macrophages treated with SJMHE1 promoted the proliferative activity of Schwann cells and the growth of DRG neuron axons. In conclusion, we found that SJMHE1 promoted peripheral nerve repair and functional regeneration through a macrophage-dependent, M2-related mechanism, indicating that schistosome-derived SJMHE1 has therapeutic potential for peripheral nerve injury.

Acknowledgements

This work was supported by the grants from the National Natural Science Foundation of China (No. 81871675 and No. 81430052), and the National Key Research and Development Program of China (MOST No: 2018YFA0507300) to Chuan Su, grants from the National Natural Science Foundation of China (No. 81871676), and the Natural Science Foundation of Jiangsu Province (No. BK20190082) to Xiaojun Chen, grants from the National Natural Science Foundation of China (No. 81871243) and the key research and development programs of Jiangsu Province (BE2017697) and the Six Talent Peaks of Jiangsu Province (WSN-009) to Xuefeng Wang, and grants from the Young Talent Development Plan of Changzhou Health Commission (CZQM2020117) and the Science and Technology Plan Project of Changzhou (CJ20200003) to Yongbin Ma.

Disclosure of conflict of interest

None.

Address correspondence to: Drs. Chuan Su and Xiaojun Chen, State Key Lab of Reproductive Medicine, Jiangsu Key Laboratory of Pathogen Biology, Department of Pathogen Biology and Immunology, Center for Global Health, Nanjing Medical University, Nanjing 211166, Jiangsu, P. R. China. E-mail: chuansu@njmu.edu.cn (CS); chenxiaojun@njmu.edu.cn (XJC); Dr. Xuefeng Wang, Department of Central Laboratory, The Affiliated Hospital of Jiangsu University, Zhenjiang 212000, Jiangsu, P. R. China. E-mail: xuefengwang@ujs.edu.cn

References

[1] Scheib J and Hoke A. Advances in peripheral nerve regeneration. Nat Rev Neurol 2013; 9: 668-676.

[2] Gordon T. Nerve regeneration in the peripheral and central nervous systems. J Physiol 2016; 594: 3517-3520.

[3] Navarro X, Vivo M and Valero-Cabre A. Neural plasticity after peripheral nerve injury and regeneration. Prog Neurobiol 2007; 82: 163-201.

[4] Bergmeister KD, Grosse-Hartlage L, Daeschler SC, Rhodius P, Bocker A, Beyersdorff M, Kern AO, Kneser U and Harhaus L. Acute and long-term costs of 268 peripheral nerve injuries in the upper extremity. PLoS One 2020; 15: e0229530.

[5] Camara-Lemarroy CR, Guzman-de la Garza FJ and Fernandez-Garza NE. Molecular inflammatory mediators in peripheral nerve degeneration and regeneration. Neuroimmunomodulation 2010; 17: 314-324.

[6] Austin PJ and Moalem-Taylor G. The neuro-immune balance in neuropathic pain: involvement of inflammatory immune cells, immune-like glial cells and cytokines. J Neuroimmunol 2010; 229: 26-50.
[7] Kim CF and Moalem-Taylor G. Detailed characterization of neuro-immune responses following neuropathic injury in mice. Brain Res 2011; 1405: 95-108.
[8] Perry VH, Brown MC and Gordon S. The macrophage response to central and peripheral nerve injury. A possible role for macrophages in regeneration. J Exp Med 1987; 165: 1218-1223.
[9] Chen P, Piao X and Bonaldo P. Role of macrophages in Wallerian degeneration and axonal regeneration after peripheral nerve injury. Acta Neuropathol 2015; 130: 605-618.
[10] Mosser DM and Edwards JP. Exploring the full spectrum of macrophage activation. Nat Rev Immunol 2008; 8: 958-969.
[11] Stratton JA, Holmes A, Rosin NL, Sinha S, Vohra M, Burma NE, Trang T, Midha R and Biernaskie J. Macrophages regulate schwann cell maturation after nerve injury. Cell Rep 2018; 24: 2561-2572, e2566.
[12] Gause WC, Rothlin C and Loke P. Heterogeneity in the initiation, development and function of type 2 immunity. Nat Rev Immunol 2020; 20: 603-614.
[13] Gieseck RL 3rd, Wilson MS and Wynn TA. Type 2 immunity in tissue repair and fibrosis. Nat Rev Immunol 2018; 18: 62-76.
[14] Kuo HS, Tsai MJ, Huang MC, Chiu CW, Tsai CY, Lee MJ, Huang WC, Lin YL, Kuo WC and Cheng H. Acid fibroblast growth factor and peripheral nerve grafts regulate Th2 cytokine expression, macrophage activation, polyamine synthesis, and neurotrophin expression in transected rat spinal cords. J Neurosci 2011; 31: 4137-4147.
[15] Rotshenker S. Wallerian degeneration: the innate-immune response to traumatic nerve injury. J Neuroinflammation 2011; 8: 109.
[16] Eming SA, Krieg T and Davidson JM. Inflammation in wound repair: molecular and cellular mechanisms. J Invest Dermatol 2007; 127: 514-525.
[17] Jia Y, Yang W, Zhang K, Qiu S, Xu J, Wang C and Chai Y. Nanofiber arrangement regulates peripheral nerve regeneration through differential modulation of macrophage phenotypes. Acta Biomater 2019; 83: 291-301.
[18] Kano F, Matsubara K, Ueda M, Hibi H and Yamamoto A. Secreted ectodomain of sialic acid-binding ig-like lectin-9 and monocyte chemoattractant protein-1 synergistically regenerate transected rat peripheral nerves by altering macrophage polarity. Stem Cells 2017; 35: 641-653.
[19] Chen P, Cescon M, Zuccolotto G, Nobbio L, Colombelli C, Filaferro M, Vitale G, Feltri ML and Bonaldo P. Collagen VI regulates peripheral nerve regeneration by modulating macrophage recruitment and polarization. Acta Neuropathol 2015; 129: 97-113.
[20] Harris NL and Loke P. Recent advances in type-2-cell-mediated immunity: insights from helminth infection. Immunity 2017; 47: 1024-1036.
[21] Dastpeyman M, Bansal PS, Wilson D, Sotillo J, Brindley PJ, Loukas A, Smout MJ and Daly NL. Structural variants of a liver fluke derived granulin peptide potently stimulate wound healing. J Med Chem 2018; 61: 8746-8753.
[22] Wang X, Zhou S, Chi Y, Wen X, Hoellwarth J, He L, Liu F, Wu C, Dhesi S, Zhao J, Hu W and Su C. CD4+CD25+ Treg induction by an HSP60-derived peptide SJMHE1 from Schistosoma japonicum is TLR2 dependent. Eur J Immunol 2009; 39: 3052-3065.
[23] Gao B and Tsan MF. Endotoxin contamination in recombinant human heat shock protein 70 (Hsp70) preparation is responsible for the induction of tumor necrosis factor alpha release by murine macrophages. J Biol Chem 2003; 278: 174-179.
[24] Ma Y, Dong L, Zhou D, Li L, Zhang W, Zhen Y, Wang T, Su J, Chen D, Mao C and Wang X. Extracellular vesicles from human umbilical cord mesenchymal stem cells improve nerve regeneration after sciatic nerve transection in rats. J Cell Mol Med 2019; 23: 2822-2835.
[25] Inserra MM, Bloch DA and Terris DJ. Functional indices for sciatic, peroneal, and posterior tibial nerve lesions in the mouse. Microsurgery 1998; 18: 119-124.
[26] Yuan H, Zhang J, Liu H and Li Z. The protective effects of resveratrol on Schwann cells with toxicity induced by ethanol in vitro. Neurochem Int 2013; 63: 146-153.
[27] Lopez-Verrilli MA, Picou F and Court FA. Schwann cell-derived exosomes enhance axonal regeneration in the peripheral nervous system. Glia 2013; 61: 1795-1806.
[28] Wang X, Li L, Wang J, Dong L, Shu Y, Liang Y, Shi L, Xu C, Zhou Y, Wang Y, Chen D and Mao C. Inhibition of cytokine response to TLR stimulation and alleviation of collagen-induced arthritis in mice by Schistosoma japonicum peptide SJMHE1. J Cell Mol Med 2017; 21: 475-486.
[29] Smallwood TB, Giacomin PR, Loukas A, Mulvenna JP, Clark RJ and Miles JJ. Helminth immunomodulation in autoimmune disease. Front Immunol 2017; 8: 453.
[30] Wu Z, Wang L, Tang Y and Sun X. Parasite-derived proteins for the treatment of allergies and autoimmune diseases. Front Microbiol 2017; 8: 2164.

[31] Vidal PM, Lemmens E, Dooley D and Hendrix S. The role of "anti-inflammatory" cytokines in axon regeneration. Cytokine Growth Factor Rev 2013; 24: 1-12.
[32] Bei F, Lee HHC, Liu X, Gunner G, Jin H, Ma L, Wang C, Hou L, Hensch TK, Frank E, Sanes JR, Chen C, Fagiolini M and He Z. Restoration of visual function by enhancing conduction in regenerated axons. Cell 2016; 164: 219-232.
[33] Zhou Y and Notterpek L. Promoting peripheral myelin repair. Exp Neurol 2016; 283: 573-580.
[34] Monk KR, Feltri ML and Taveggia C. New insights on Schwann cell development. Glia 2015; 63: 1376-1393.
[35] Kigerl KA, Gensel JC, Ankeny DP, Alexander JK, Donnelly DJ and Popovich PG. Identification of two distinct macrophage subsets with divergent effects causing either neurotoxicity or regeneration in the injured mouse spinal cord. J Neurosci 2009; 29: 13435-13444.
[36] Mokarram N, Merchant A, Mukhatyar V, Patel G and Bellamkonda RV. Effect of modulating macrophage phenotype on peripheral nerve repair. Biomaterials 2012; 33: 8793-8801.
[37] Zhan C, Ma CB, Yuan HM, Cao BY and Zhu JJ. Macrophage-derived microvesicles promote proliferation and migration of Schwann cell on peripheral nerve repair. Biochem Biophys Res Commun 2015; 468: 343-348.

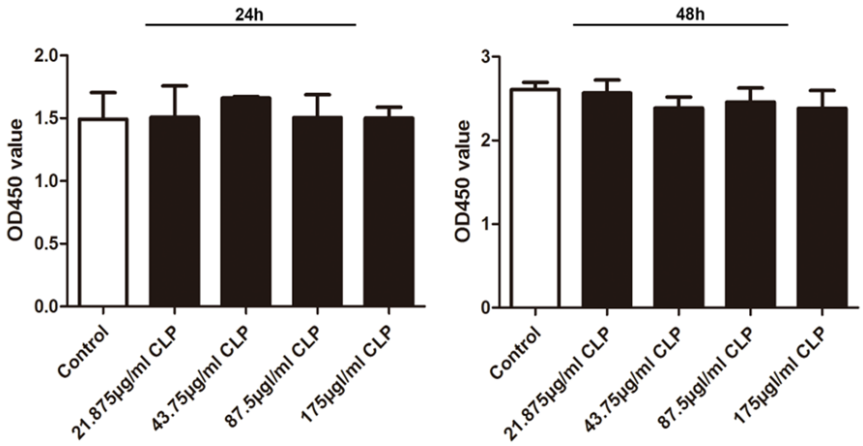

Supplementary Figure 1. Chlorophosphate liposomes had no direct effect on the proliferation of Schwann cells. The CCK8 assay was performed to analyzed Schwann cell proliferation follow administration of different concentrations of chlorophosphonate liposomes. CLP, chlorophosphate liposome. Groups treated with CLPs at different concentrations *vs* the control group; n = 3 for each group; *P*>0.05 indicates no statistical significance (ANOVA). The data are presented as the mean ± SEM.

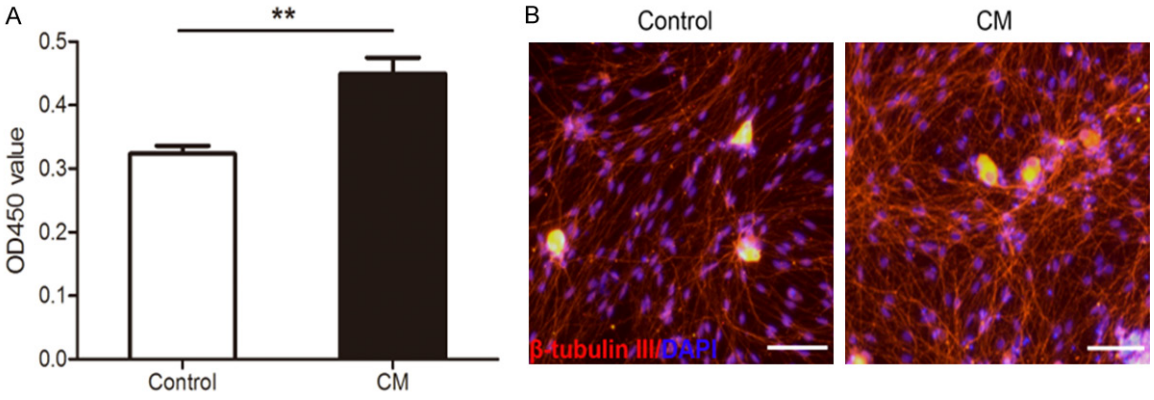

Supplementary Figure 2. Treatment with macrophage-conditioned medium (CM) and SJMHE1 promotes the proliferative activity of Schwann cells and an increase in density of DRG neuron axons. (A) Assessment of Schwann cell proliferation by the CCK8 assay. (B) Immunofluorescence staining for β-tubulin III (red) in DRG neurons. DAPI (blue)-stained nuclei. Scale bar = 100 μm. The CM group *vs* the control group; n = 3 for each group; **P<0.01 (Student's *t* test). The data are presented as the mean ± SEM.